Solid-State Motion Hot Paper

International Edition: DOI: 10.1002/anie.201813554
German Edition: DOI: 10.1002/ange.201813554

Spontaneous and Fast Molecular Motion at Room Temperature in the Solid State

*Parvej Alam[+], Nelson L. C. Leung[+], Yanhua Cheng, Haoke Zhang, Junkai Liu, Wenjie Wu, Ryan T. K. Kwok, Jacky W. Y. Lam, Herman H. Y. Sung, Ian D. Williams, and Ben Zhong Tang**

Abstract: *The development of molecular machines requires new building blocks which are easy to characterize and visualize to realize a complexity comparable to their natural counterparts such as biological enzymes. Furthermore, with the desire to build functional nanobots capable of navigating living organisms, it is necessary that the building blocks show mobility even in the solid state. Herein we report a system which is emissive in the amorphous state but is non-fluorescent in the crystalline state due to the formation of extensive π-π interactions. This dual nature could be exploited for easy visualization of its solid-state molecular rearrangement. The emission of the amorphous film was quenched as the molecules spontaneously formed π-π interactions even in the solid state. Scratching the non-emissive film destroyed the interactions and restored the emission of the film. The emission quickly disappeared with an average lifetime of 20 s as the compound reformed the π-network even at room temperature.*

Nature has created an incredible body of molecular machines (MMs) perfectly tailored for biochemical pathways and processes necessary for life.[1] From single cellular organisms to complex life forms, these MMs break down, build up, or repair other molecules and even other MMs. One far-off goal is to design synthetic MMs with similar or even more complex functions than those of natural systems. To achieve such a task, a toolbox of multifaceted knowledge for molecular machinery is needed. Luckily, systems such as catenanes,[2] rotaxanes,[3] molecular switches,[4] or molecular rotors,[5] from Sauvage,[6] Stoddart,[7] Feringa,[8] Credi,[9] Leigh,[10] Balzani,[11] and many others,[12] fill the toolbox necessary for developing MMs. However, the tools currently available at our disposal are far from enough to build the desired complex machines. One of the challenges that needs to be overcome to bring such aspirations to fruition is that we need even more fundamental techniques, knowledge, and systems. In addition, due to the size and nature of MMs, the characterization of their motions or states is also a challenging task. Currently, one of the most successful ways to characterize MMs is through powerful NMR spectroscopy.[2–5,13] Peak shifts and differences reflect the changes that the molecular units undergo. Though NMR spectroscopy provides an accurate snapshot of the current state of the MM, it is limited to single states or frames. It is difficult to continuously monitor real-time changes of MMs via NMR spectroscopy.

The development of new systems with easily detectable optical, electronic, and/or mechanical outputs would greatly facilitate monitoring state changes of MMs.[10a] Indeed, researchers have started to incorporate specific moieties into MMs to provide such properties. The molecular elevator[7b] reported by Stoddart and Credi can, in addition to NMR characterization, also be monitored using electrochemistry as well as absorption and fluorescence spectroscopy. Although not all designs can incorporate such a functionality with ease, systems with additional means of examination are of advantage. Furthermore, many MM systems have been designed and studied in solution. While solution-based MMs are good for an initial study and verification, researchers recognize that there is also a large demand for MMs to be used in other microenvironments.[14] For example, one vision is to design MMs as theranostic nanobots in the body. To achieve such a goal, the MMs will need to work in environments like tissues, soft matter interfaces, and even in the solid state. In this vein, some work has already been done such as attaching rotaxanes onto solid surfaces.[14] More recently, nanocars[12,15] have been shown to move unidirectionally on solid substrates. The unidirectional motion could be tracked using scanning tunneling microscopy. These successes inspire future research.

In this work, we focused on combining several ideas into one single system: a new building block capable of solid-state motion which could be used in the future for MMs with easy optical output for signaling. The phenomenon of aggregation-induced emission (AIE) is well suited for such a task. AIE describes a general phenomenon where molecules are non-luminescent in solution but emit intensely when they bind to molecules, analytes, or substrates.[16] The restriction of intramolecular motions (RIM) has been identified as the cause of

[*] Dr. P. Alam,[+] N. L. C. Leung,[+] Dr. Y. Cheng, Dr. H. Zhang, J. Liu, W. Wu, Dr. R. T. K. Kwok, Dr. J. W. Y. Lam, Dr. H. H. Y. Sung, Prof. I. D. Williams, Prof. B. Z. Tang
Department of Chemistry, Hong Kong Branch of Chinese National Engineering Research Center for Tissue Restoration and Reconstruction and Institute for Advanced Study, The Hong Kong University of Science and Technology
Clear Water Bay, Kowloon, Hong Kong (China)
E-mail: tangbenz@ust.hk
Prof. B. Z. Tang
HKUST-Shenzhen Research Institute
No. 9 Yuexing 1st Rd, South Area, Hi-tech Park, Nanshan, Shenzhen 518057 (China)
Prof. B. Z. Tang
Centre for Aggregation-induced emission, SCUT-HKUST Joint Research Laboratory, State Key Laboratory of Luminescent Materials and Devices, South China University of Technology
Guangzhou 510640 (China)
[+] These authors contributed equally to this work.
Supporting information and the ORCID identification number(s) for the author(s) of this article can be found under: https://doi.org/10.1002/anie.201813554.

the AIE phenomenon which prevents the loss of excited-state energy through non-radiative relaxation pathways by molecular motions.[17] The RIM mechanism has been widely used to explain the AIE effects of many systems and has created a successful platform for designing a new AIE luminogens (AIEgens) for biomedical imaging and theranostic applications,[18] chemical sensors,[19] monitoring and visualizing physical processes,[20] and much more.[16a]

In typical AIEgens, bulky rotors prevent the formation of π-π interactions which quench light emission. On the other hand, π-π interactions can be a strong driving force for molecular packing. We explored the possibility of combining pyrene,[21] a well-known molecule with ease in forming π-π interactions, with a phenyl rotor to generate an AIEgen with strong intermolecular interactions. The synthesized AIEgen, (*E*)-2-[(pyren-1-ylimino)methyl]phenol (PIP) (Figure 1),

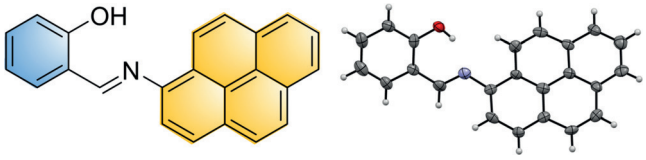

Figure 1. (Left) Molecular structure of (*E*)-2-[(pyren-1-ylimino)methyl]-phenol (PIP). (Right) Thermal ellipsoid (50%) plot of PIP.

shows AIE activity. Interestingly, in crystal form, it exhibits drastically quenched emission and analysis by single-crystal X-ray diffraction showed that this was caused by the formation of an extensive π-network herringbone structure. The π-network was able to regenerate spontaneously after external disruption at room temperature in the solid state, during which observable change in the emission was detected. Disrupting the π-interactions turns on light emission of the molecule and with an average lifetime of about 20 s, the molecule becomes non-fluorescent again due to the reformation and regeneration of the emission-quenching π-network.

PIP was synthesized by a simple condensation reaction of 1-aminopyrine and salicylaldehyde.[22] The detailed procedures are described in the Supporting Information (Scheme S1). The chemical structure of PIP was confirmed by standard spectroscopic techniques including NMR, HRMS, and SXRD (Figure S1). Light-yellow colored crystals of PIP were obtained by slow evaporation of a solution of it in ethanol. The quantum yield (Φ_F) of the PIP crystals was too low to be measured but was found to be 1.15% in a 1 wt% doped poly(methyl methacrylate) film with an emission maximum at 550 nm.

There are two different motifs in the crystal packing: 1) a head-to-head herringbone configuration (Figure 2A) and 2) a dimeric head-to-tail configuration (Figure 2B). In the herringbone motif, two neighboring molecules interact with carbon–carbon distances of 3.279 Å to 3.350 Å. In the head-to-tail dimers, the pyrene ring of one PIP unit is stacked on the phenyl ring of a second molecule with carbon–carbon distances of 3.299 Å to 3.393 Å. The layers of herringbone motifs are connected to each other via head-to-tail dimers (Figure 2C). The presence of strong π-π interactions between

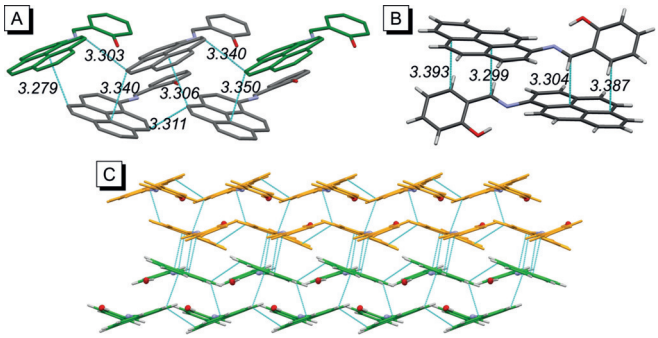

Figure 2. Intermolecular π-π interactions in a single-crystal X-ray structure of PIP with A) head-to-head herringbone packing and B) head-to-tail dimers. C) Head-to-head herringbone layers (yellow or green) and their connection by head-to-tail dimers (between yellow and green units).

PIP molecules plays an important role in accessing non-radiative channels to quench emission in the crystal state. For comparison, emissive PIP aggregates formed in a ACN/H_2O mixture with $f_w = 90\%$ (Supporting Information, Figures S2 and S3) were collected and analyzed after freeze-drying by powder X-ray diffraction (PXRD) and electron diffraction. Both techniques indicated that the emissive aggregates were amorphous in nature (Figure S4). PIP was also examined under different solution concentrations by ^{1}H NMR spectroscopy (Figure S5), and the gradual increase in the shielding effect of the resonance peaks with increasing concentration suggested the formation of π-π interactions. This observation may help explain the formation of a π-network in PIP crystals and indicates that the attractive π-π interactions endow PIP with a natural tendency to aggregate. Furthermore, cracking the crystals generated emissive fracture lines (Supporting Information, Figure S6), likely due to the disruption of the π-π interactions at these locations. The on/off emission behavior of the amorphous and crystalline state proved to be a useful tool for visualizing different environments and states.

A fascinating solid-state phenomenon was observed in PIP: its molecules will spontaneously rearrange themselves to form a solid with higher crystallinity but no light emission under excitation. Stimuli-responsive turn-on emission can then be detected from PIP, after which the PIP film will convert to its non-emissive form even at room temperature. To gain a deeper understanding of this phenomenon, PXRD analysis of the PIP powder was carried out (Supporting Information, Figure S7A). The PXRD diffraction showed intense diffraction peaks, revealing the crystalline nature of the powder. The peaks corresponded to the simulated powder pattern derived from the single-crystal XRD structure. Surprisingly, the PXRD diffraction obtained after strong grinding showed intense diffraction peaks with similar peak positions compared to fresh PIP. One explanation is that during the time between grinding and immediate sample preparation for the PXRD measurement, the molecules were already recrystallized.

To provide evidence for this, time-dependent PL spectroscopy was performed on a drop-cast thin film of PIP on quartz glass. As shown in Figure S8 (Supporting Information),

a continuous decrease in the PL intensity was observed. The observed continuous PL quenching in this process was ascribed to the formation of π-π interactions resembling those in the crystal packing rather than photobleaching. The PXRD patterns of fresh and overnight neat films support this (Figure S7 B). Compared to the pattern of the fresh neat film, more crystalline peaks could be seen after 12 h. As a control, a drop-cast polystyrene (PS) film doped with 1 wt % PIP was also scanned under the same conditions. However, no detectable drop in PL intensity was detected (Figure S8 B, C). The fact that the rigid PS film with a low concentration of PIP showed consistent emission while the neat film exhibited quenched emission ruled out photobleaching as the quenching mechanism. It also suggests that without a rigid environment to hinder the molecular motion, PIP could form π-π interactions in the solid state. The time-dependent emission quenching of PIP was also observed on other substrates, such as cellulose paper and weighing paper, with much pronounced results. For example, after a few drops of a 10 μM DCM solution of PIP were put onto cellulose paper or weighing paper, a bright emission could be seen after the evaporation of DCM. After being kept in the dark overnight, the bright emission was quenched. Since the weighing paper showed the highest contrast, further study was done on this substrate.

When the non-emissive film on weighing paper was scratched with a spatula, the scratched area showed an intense yellow emission. Quickly, the bright emissive areas returned to their original non-emissive state. The emission turn-on property by scratching and fast self-recovery were highly reversible and monitored by PL measurements (Figure 3 and video in the Supporting Information). The PL turn-on and -off features of the sample were measured at 550 nm and the calculated lifetime for the self-recovery was about 20 s.

Because the fresh film was highly emissive, this suggests that in the beginning, PIP lacks π-π interactions. During a time of 12 h, emission quenching starts to occur as π-π interactions form between molecules. Scratching by a spatula disrupts the π-π interactions, resulting in an emission turn-on, and the fast self-recovery indicates the easy reformation of the quenching π-π interactions. The repeatability of both the dark and bright states of PIP suggests a physical phenomenon

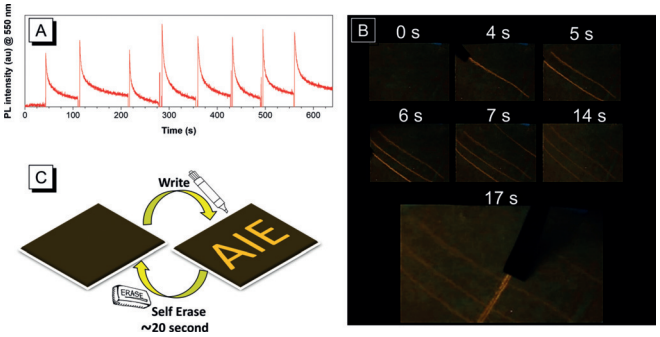

Figure 3. A) Fast and spontaneous response of PIP after scratching captured by a PL intensity measurement. B) Visual demonstration of the fast turn-on/off fluorescence processes. C) Schematic representation of the writing–erasing processes.

that the molecules move within the film to form or reform the π-π interactions. A control experiment was also performed by examining the emission of a fresh and an overnight film on weighing paper. The two films were irradiated side-by-side under a handheld UV lamp at 365 nm. While the fresh film was yellow-emissive, the overnight film was completely non-fluorescent. Scratching the overnight film turned on the emission process, which quickly recovered to the initial non-emissive state. This observation was similar to the one shown in Figure 3 B. In contrast, the fresh film showed no sign of emission change, which suggests that photobleaching was not the cause of the fast and spontaneous quenching. We attempted to collect the PXRD patterns of the films on the weighing papers, but no peaks were detected for both the emissive and non-emissive films. Since diffraction patterns are formed by X-ray scattering on ordered arrangements of atoms, it seems that it is difficult for PIP to form regularly packed crystallites on weighing paper that produce detectable patterns.

To test the hypothesis of molecular motion in the solid state, PL measurements of the fresh PIP film were taken and compared after storage at different temperatures (−20 °C, 25 °C and 60 °C) (Supporting Information, Figure S9). The PIP film stored at 60 °C showed a 63 % reduction in PL intensity in only about 5 min. The sample kept at room temperature showed a 38 % reduction of the PL intensity in 30 min (0.5 h). For the sample stored at −20 °C, only 20 % PL quenching was found after 6 h and the PL intensity only decreased to 50 % of its original value after 21 h. Molecular motions are highly temperature-dependent and the mobility of the molecules decreases proportionally to the temperature. This experiment suggests that the molecular motion of PIP is highly suppressed at low temperatures.

To gain more insight into the mechanism of the fluorescence on/off property, theoretical calculations using hybrid quantum mechanics and molecular mechanics (QM/MM) were carried out. The single crystal was used as the initial geometry for structural optimization. The geometry for the monomer, dimer, and tetramer optimizations were constructed based on the respective single-crystal arrangement in the supercell with 69 surrounding molecules. The calculated energy gap decreased as the number of molecules increased, from 3.201 eV in the monomer to 2.533 eV in the tetramer (Figure 4). The change in the energy gap is due to the gradual destabilization and stabilization of the highest occupied molecular orbital (HOMO) and the lowest unoccupied molecular orbital (LUMO), respectively, when the number of molecules increases. This result is consistent with the experimental absorption spectrum of PIP, where the onset wavelength was found to be red-shifted in thin films compared to solution (Supporting Information, Figure S11 A). The single-point energy calculations provide insight into the driving force of the fluorescence on/off process. The total energy of the system was found to be more stabilizing with increasing number of molecules. The calculation demonstrated that the dimer experiences an additional stabilization of 1.8 % compared to its monomer equivalent while the tetramer experiences an additional stabilization of 2.5 %. This stabilization effect would be expected to increase

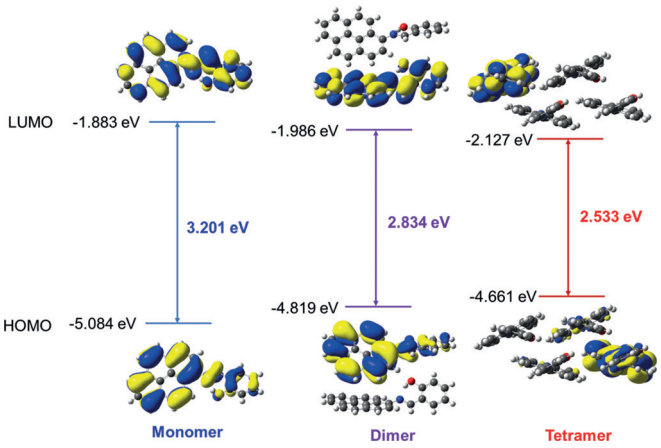

Figure 4. Frontier molecular orbitals of the monomer, dimer, and tetramer and the corresponding HOMO and LUMO energies.

when more intermolecular herringbone interactions form in the presence of more molecules. This becomes a driving force for the fast and spontaneous formation of a π-network and is also the cause of the non-emissive nature of PIP in the solid state. By exploiting the emission of PIP based on the presence or absence of π-π interactions, the visualization of microphase separations in polymer blends became feasible with a high fluorescence on/off contrast (see Supporting Information).

In this work, an AIE-active molecule exhibiting controllable emission was reported. PIP is emissive in the amorphous state while it is non-emissive in the crystalline state due to the formation of extensive π-π interactions. PIP molecules demonstrated the ability to rearrange themselves to form π-π interactions even in the solid state. The formation of π-π interactions was driven by stabilization enhancement stemming from intermolecular interactions and can be exploited for the visualization of molecular motions. Realization of the π-network formation resulted in easily observable emission quenching. The spontaneous motion was a repeatable process and could be observed by simply scratching the surface to disrupt the π-π interactions, leading to an emission turn-on. In an average lifetime of about 20 s, the π-network reformed, resulting in emission quenching. The emission quenching in the solid state was temperature-dependent, which became severe with increasing temperature due to the enhanced molecular motions that lead to the reformation of the π-network. The system reported here demonstrates spontaneous solid-state molecular motion and exemplifies the use of luminescence to monitor such motions. The ability for solid-state motion will become pivotal in the development of the next generation of molecular machines. It is our hope that this work will inspire other researchers by showing how intermolecular forces can be exploited for solid-state motion. Further investigation on the solid-state motion of PIP and other possible systems are in progress in our lab.

Acknowledgements

This work was financially supported by the National Science Foundation of China (21788102), the Research Grants Council of Hong Kong (16308016, 16305015, 16305518, C2014-15G, C6009-17G and A-HKUST605/16), the Innovation and Technology Commission (ITC-CNERC14SC01 and ITC/254/17), and the Science and Technology Plan of Shenzhen (JCYJ20160229205601482 and JCYJ20170818113602462).

Conflict of interest

The authors declare no conflict of interest.

Keywords: aggregation-induced emission · ESIPT · molecular motion · polymer microphase visualization

How to cite: *Angew. Chem. Int. Ed.* **2019**, *58*, 4536–4540
Angew. Chem. **2019**, *131*, 4584–4588

[1] a) K. Mislow, *Chemtracts: Org. Chem.* **1989**, *2*, 151–174; b) V. Balzani, A. Credi, F. M. Raymo, J. F. Stoddart, *Angew. Chem. Int. Ed.* **2000**, *39*, 3348–3391; *Angew. Chem.* **2000**, *112*, 3484–3530; c) E. R. Kay, D. A. Leigh, *Angew. Chem. Int. Ed.* **2015**, *54*, 10080–10088; *Angew. Chem.* **2015**, *127*, 10218–10226; d) M. Schliwa, G. Woehlke, *Nature* **2003**, *422*, 759.

[2] a) N. H. Evans, P. D. Beer, *Chem. Soc. Rev.* **2014**, *43*, 4658–4683; b) G. Gil-Ramírez, D. A. Leigh, A. J. Stephens, *Angew. Chem. Int. Ed.* **2015**, *54*, 6110–6150; *Angew. Chem.* **2015**, *127*, 6208–6249.

[3] a) M. Xue, Y. Yang, X. Chi, X. Yan, F. Huang, *Chem. Rev.* **2015**, *115*, 7398–7501; b) G. Wenz, B.-H. Han, A. Müller, *Chem. Rev.* **2006**, *106*, 782–817.

[4] a) H. Tian, Q.-C. Wang, *Chem. Soc. Rev.* **2006**, *35*, 361–374; b) B. L. Feringa, R. A. van Delden, N. Koumura, E. M. Geertsema, *Chem. Rev.* **2000**, *100*, 1789–1816.

[5] a) G. S. Kottas, L. I. Clarke, D. Horinek, J. Michl, *Chem. Rev.* **2005**, *105*, 1281–1376; b) S. Kassem, T. van Leeuwen, A. S. Lubbe, M. R. Wilson, B. L. Feringa, D. A. Leigh, *Chem. Soc. Rev.* **2017**, *46*, 2592–2621.

[6] a) C. O. Dietrich-Buchecker, J. P. Sauvage, J. P. Kintzinger, *Tetrahedron Lett.* **1983**, *24*, 5095–5098; b) C. O. Dietrich-Buchecker, J. P. Sauvage, J. M. Kern, *J. Am. Chem. Soc.* **1984**, *106*, 3043–3045.

[7] a) P. L. Anelli, N. Spencer, J. F. Stoddart, *J. Am. Chem. Soc.* **1991**, *113*, 5131–5133; b) J. D. Badjić, V. Balzani, A. Credi, S. Silvi, J. F. Stoddart, *Science* **2004**, *303*, 1845.

[8] a) D. Roke, S. J. Wezenberg, B. L. Feringa, *Proc. Natl. Acad. Sci. USA* **2018**, *115*, 9423; b) W. R. Browne, B. L. Feringa, *Nat. Nanotechnol.* **2006**, *1*, 25.

[9] a) M. Baroncini, L. Casimiro, C. de Vet, J. Groppi, S. Silvi, A. Credi, *ChemistryOpen* **2018**, *7*, 169–179; b) V. Balzani, M. Clemente-Leon, A. Credi, B. Ferrer, M. Venturi, A. H. Flood, J. F. Stoddart, *Proc. Natl. Acad. Sci. USA* **2006**, *103*, 1178–1183.

[10] a) S. Erbas-Cakmak, D. A. Leigh, C. T. McTernan, A. L. Nussbaumer, *Chem. Rev.* **2015**, *115*, 10081–10206; b) L. Zhang, V. Marcos, D. A. Leigh, *Proc. Natl. Acad. Sci. USA* **2018**, *115*, 9397–9404.

[11] a) R. Ballardini, V. Balzani, A. Credi, M. T. Gandolfi, M. Venturi, *Acc. Chem. Res.* **2001**, *34*, 445–455; b) V. Balzani, A. Credi, M. Venturi, *Chem. Soc. Rev.* **2009**, *38*, 1542–1550.

[12] a) C. J. Villagómez, T. Sasaki, J. M. Tour, L. Grill, *J. Am. Chem. Soc.* **2010**, *132*, 16848–16854; b) Y. Shirai, J.-F. Morin, T. Sasaki, J. M. Guerrero, J. M. Tour, *Chem. Soc. Rev.* **2006**, *35*, 1043–1055.

[13] R. Rosenzweig, L. E. Kay, *J. Am. Chem. Soc.* **2016**, *138*, 1466–1477.

[14] K. Ariga, T. Mori, J. P. Hill, *Soft Matter* **2012**, *8*, 15–20.

[15] a) Y. Shirai, A. J. Osgood, Y. Zhao, K. F. Kelly, J. M. Tour, *Nano Lett.* **2005**, *5*, 2330 – 2334; b) T. Kudernac, N. Ruangsupapichat, M. Parschau, B. Maciá, N. Katsonis, S. R. Harutyunyan, K.-H. Ernst, B. L. Feringa, *Nature* **2011**, *479*, 208.
[16] a) J. Mei, N. L. C. Leung, R. T. K. Kwok, J. W. Y. Lam, B. Z. Tang, *Chem. Rev.* **2015**, *115*, 11718 – 11940; b) Y. N. Hong, J. W. Y. Lam, B. Z. Tang, *Chem. Soc. Rev.* **2011**, *40*, 5361 – 5388.
[17] H. Nie, K. Hu, Y. Cai, Q. Peng, Z. Zhao, R. Hu, J. Chen, S.-J. Su, A. Qin, B. Z. Tang, *Mater. Chem. Front.* **2017**, *1*, 1125 – 1129.
[18] a) D. Ding, K. Li, B. Liu, B. Z. Tang, *Acc. Chem. Res.* **2013**, *46*, 2441 – 2453; b) X. Y. Zhang, K. Wang, M. Y. Liu, X. Q. Zhang, L. Tao, Y. W. Chen, Y. Wei, *Nanoscale* **2015**, *7*, 11486 – 11508; c) G. S. Hong, A. L. Antaris, H. J. Dai, *Nat. Biomed. Eng.* **2017**, *1*, 22.
[19] H. N. Kim, Z. Q. Guo, W. H. Zhu, J. Yoon, H. Tian, *Chem. Soc. Rev.* **2011**, *40*, 79 – 93.
[20] a) W. J. Guan, W. J. Zhou, C. Lu, B. Z. Tang, *Angew. Chem. Int. Ed.* **2015**, *54*, 15160 – 15164; *Angew. Chem.* **2015**, *127*, 15375 – 15379; b) Z. K. Wang, J. Y. Nie, W. Qin, Q. L. Hu, B. Z. Tang, *Nat. Commun.* **2016**, *7*, 8.
[21] Z. Xu, N. J. Singh, J. Lim, J. Pan, H. N. Kim, S. Park, K. S. Kim, J. Yoon, *J. Am. Chem. Soc.* **2009**, *131*, 15528 – 15533.
[22] a) Y. Zhang, Z.-H. Lu, *Mater. Chem. Phys.* **2000**, *63*, 188 – 195; b) D. A. Safin, M. Bolte, Y. Garcia, *CrystEngComm* **2014**, *16*, 8786 – 8793.
[23] a) J. L. White, S. H. Bumm, *Encyclopedia of Polymer Blends*, Wiley-VCH, Weinheim, **2016**; b) L. A. Goettler, J. J. Scobbo in *Polymer Blends Handbook* (Eds.: L. A. Utracki, C. A. Wilkie), Springer Netherlands, Dordrecht, **2014**, pp. 1433 – 1458; c) D. R. Paul in *Functional Polymers* (Eds.: D. E. Bergbreiter, C. R. Martin), Springer US, Boston, **1989**, pp. 1 – 18.
[24] T. Han, C. Gui, J. W. Y. Lam, M. Jiang, N. Xie, R. T. K. Kwok, B. Z. Tang, *Macromolecules* **2017**, *50*, 5807 – 5815.

Manuscript received: November 28, 2018
Revised manuscript received: January 22, 2019
Accepted manuscript online: January 28, 2019
Version of record online: February 28, 2019

